

Supporting Information

High-Accuracy Measurement of Crystalline Orientation of Anisotropic Two-Dimensional Materials using Photothermal Detection

Xiaoguang Gao, Guoxing Chen, Dekang Li, Xiaokuan Li, Zhibo Liu*, Jianguo Tian

The Key Laboratory of Weak Light Nonlinear Photonics, Ministry of Education, Teda Applied Physics

Institute and School of Physics, Nankai University, Tianjin 300071, China

Correspondence and requests for materials should be addressed to Z.L. (email: liuzb@nankai.edu.cn).

Table of Contents

S1 Experimental setup of polarization-dependent reflection and absorption of BP

S2 The tri-layer system model and transfer-matrix method for calculations

S3 Preparation of materials and methods

S4 Explore the impact of laser power on the samples in PTD and polarized Raman techniques.

S5 Reflectance and transmission spectra of BP and ReS2 samples on different substrates.

Supporting Information S1

Experimental setup of polarization-dependent reflection and absorption of BP

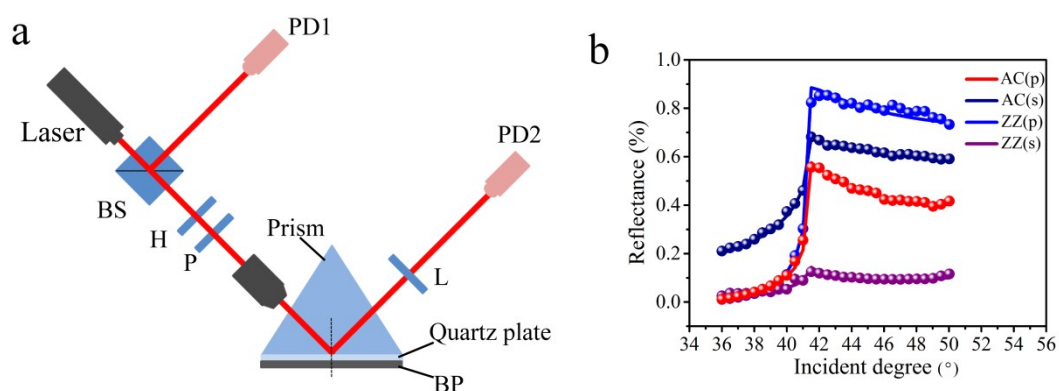


Figure S1. Exploration on polarization-dependent optical reflection of BP samples. **(a)** Schematic of the experimental setup. BS, beam splitter; H, half-wave plate; P, a polarizer; PD, photodetectors. **(b)** Plots of incident angle-dependent reflectance of BP in tri-layer system. The four curves correspond to s- and p-polarized incident beams and different incident plane along different crystal orientations AC and ZZ respectively.

As depicted in **Figure S1a**, the related experimental setup has been developed to measure the polarization-dependent reflection of BP. The probe beam at 632.8 nm from He-Ne laser is split into incident and reference beam by a beam splitter. The reference beam is used to monitor the power variation of laser to reduce the experimental error. After passing through a half-wave plate and a polarizer, the incident beam reaches a prism fixed on a rotation stage and has interactions with BP along the different crystal orientation ZZ and AC respectively. PD1 and PD2 are the two detector of a dual-channel power meter. PD1 monitors the instantaneous fluctuations of the laser energy; PD2 measures the final light reflected by the tri-layer structure.

The BP samples is exfoliated on the substrate of the quartz. The tri-layer system includes prism, BP and air. The plots of incident angle-dependent reflectance of s and p-polarized are illustrated in **Figure S1b**. The black phosphorus is a biaxial crystal, the dielectric constants along its three principle crystal axes are different. We found that when the incident plane is along AC direction, the reflection of s-polarized is greater than p-polarized light. When the incident plane is along the ZZ direction, the situation is exactly the opposite. And BP samples have the property of polarization-dependent reflection, regardless of the incident plane along the AC or ZZ

direction. The PTD adopts the situation that angle of incidence is equal to the critical angle to detect intensity change in *s*- and *p*-polarized caused by pump beam.

Supporting Information S2

The tri-layer system model and transfer-matrix method for calculations

Due to its simplicity and facility, the optical transfer matrix can be used for quantitative calculations of the reflection and transmission multi-dielectric layers.^{1, 2} Based on the classical electrodynamics simulation, the reflectance of tri-layer structure could be obtained for *s*- and *p*-polarized incident beam. The tri-layer structure consisted of BP sandwiched between two dielectrics, and the incident plane of light was assumed to be *x*, *z*-plane in medium 1 with an incident angle α . The relationship between the reflectivity, transmission, and absorption of transverse electric (TE) mode is given by Eq. (1).

$$\begin{bmatrix} i \\ r \end{bmatrix} = \begin{bmatrix} 1 + \frac{k_{pz}}{k_{1z}}\gamma_{1p} & \left(1 - \frac{k_{pz}}{k_{1z}}\gamma_{1p}\right)e^{ik_{pz}d_1} \\ 1 - \frac{k_{pz}}{k_{1z}}\gamma_{1p} & \left(1 - \frac{k_{pz}}{k_{1z}}\gamma_{1p}\right)e^{ik_{pz}d_1} \end{bmatrix} \begin{bmatrix} \left(1 + \frac{k_{2z}}{k_{pz}}\gamma_{p2}\right)e^{-ik_{pz}d_1} \\ 1 - \frac{k_{2z}}{k_{pz}}\gamma_{p2} \end{bmatrix} t$$

where the subscripts 1, *p* and 2 represent the medium 1, BP and medium 2, respectively. k_z is the component in the *z*-direction of medium wave-vector.

The relative permittivity and relative permeability are denoted as ϵ_i and μ_i , and $\gamma_{1p} = \mu_1/\mu_p$, $\gamma_{p2} = \mu_p/\mu_2$. Here, $k_0 = 2\pi/\lambda_0$ is the vacuum wavelength, $k_x = n_1k_0\sin\alpha$, $k_{1z} = \sqrt{n_1^2k_0^2 - k_x^2}$, $k_{gz} = \sqrt{n_p^2k_0^2 - k_x^2}$, and $k_{2z} = \sqrt{n_2^2k_0^2 - k_x^2}$. For transverse magnetic (TM) mode, a similar formula can be constructed if the aforementioned factor γ was changed to $\gamma_{1p} = \epsilon_1/\epsilon_p$, $\gamma_{p2} = \epsilon_p/\epsilon_2$. Then the transmittance (*T*), reflectance (*R*) and absorption (*A*) can be obtained using Eq. (2). $\begin{bmatrix} i \\ r \end{bmatrix} = M_1M_2t$, $R = |r/i|^2 = M_2M_2^*/M_1M_1^*$. For TM waves, the reflectivity and transmission can immediately be calculated by interchanging ϵ and $-\mu$ in Eq. (2).

Supporting Information S3

Preparation of materials and methods

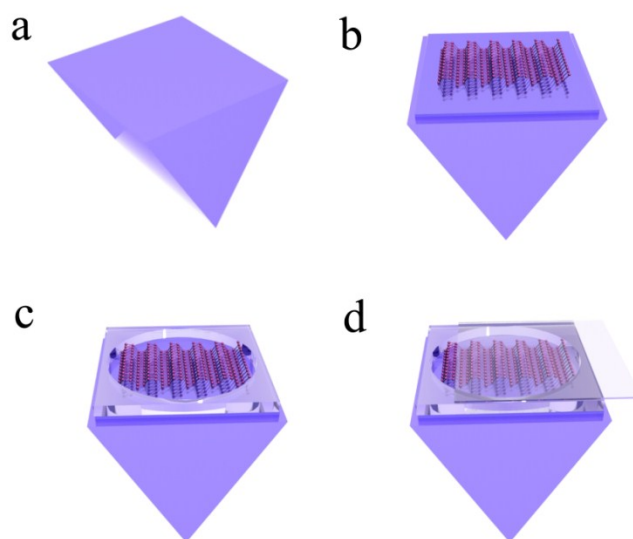


Figure S3. The preparation of materials and methods involved in **Figure 1d**. **(a)** A prism is made of K9 glasses. **(b)** The BP samples is exfoliated on the substrate of the quartz plate. **(c)** The channel is made by PDMS. **(d)** The photothermal media is injected and packaged using covership.

As displayed in **Figure S3a**, the prism adopted in the PTD experiments is made of K9 glass. The BP has been exfoliated from bulk BP crystals on plate of K9 glass. They are combined with machining solution as **Figure S3b**. Then we made preparation of channel to package the photothermal media in **Figure S3c**. Poly (dimethylsiloxane) (PDMS) was adopted to make channel in experiments due to the its chemically stable and flexible. The specific process is as follows. We weighed the Sylgard 184 silicone elastomer base and Sylgard 184 elastomer curing agent according to the ratio 10:1, respectively. The mixture is mixed well by stirring . Then the mixture was plased in a vacuum oven to remove air bubbles in it. Half an hour later, the liquid mixture was poured into petri dishes. The dishes were plased in drying oven and heated to solidify the liquid. Then remove the center of the PDMS with a mold to encapsulate the ethanol. In PTD techinque, we select the ethanol as photothermal media, and then cover with a coverslip to prevent the generation of bubbles and the the volatilization of alcohol in **Figure S3d**.

Supporting Information S4

Explore the impact of laser power on the samples in PTD and polarized Raman techniques.

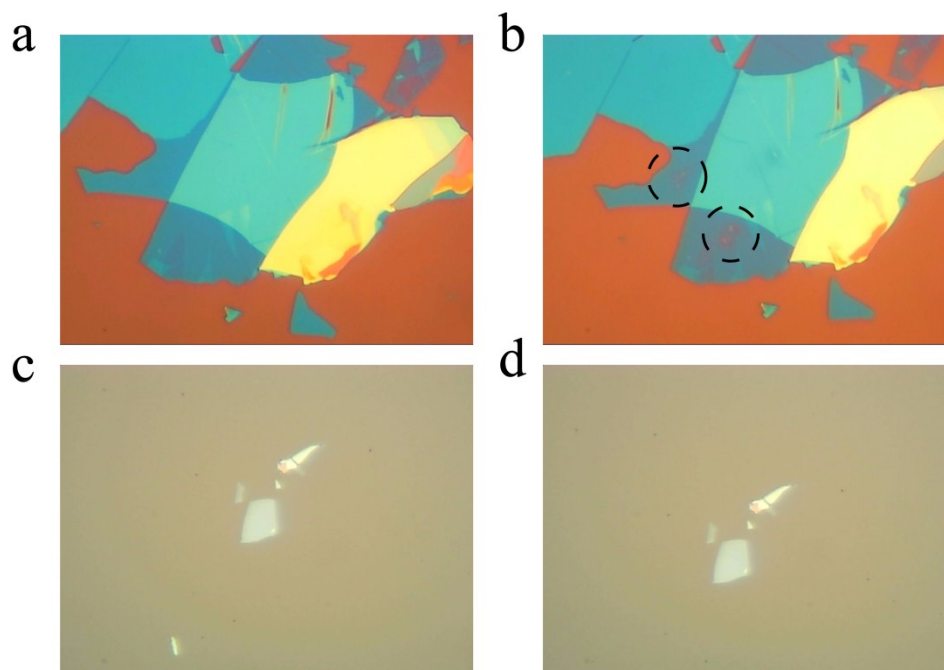


Figure S4. The comparison of BP samples before and after the PTD and polarized Raman experiments. **(a)-(b)** The comparison of BP samples used in polarized Raman experiment. **(c)-(d)** The comparison of BP samples used in PTD technique.

Figure S4a-4b illustrates the BP samples used in polarized Raman experiments. The optical images of BP with substrate of oxide-capped silicon correspond to the samples before and after Raman experiment, respectively. As depicted in **Figure S4a**, the BP samples are uniform and no oxidized degradation could be observed. Considering the situation BP samples suffer from chemical degradation in ambient conditions, the power of incident beam used in the Raman experiments is as low as 1 mW, which also makes the Raman signal weak, especially when the samples are on transparent substrate. But even so, we can still observe that BP samples suffer from chemical degradation in ambient condition due to laser irradiation as dashed line in **Figure S4b**. **Figure S4c-4d** displays the BP samples used in PTD technique. The optical images of BP with substrate of quartz correspond to the samples before and after the PTD experiment, respectively. We have mentioned that PTD is a high-sensitivity technique. The power of pump and probe beams used in experiment is as low as 30 μ W, but the photothermal signal is still strong. Compared with Raman technique, the BP samples do not suffer from chemical degradation due to the extremely low laser power in PTD experiments, which is also a very important merit.

Supporting Information S5

Reflectance and transmission spectra of BP and ReS₂ samples on different substrates.

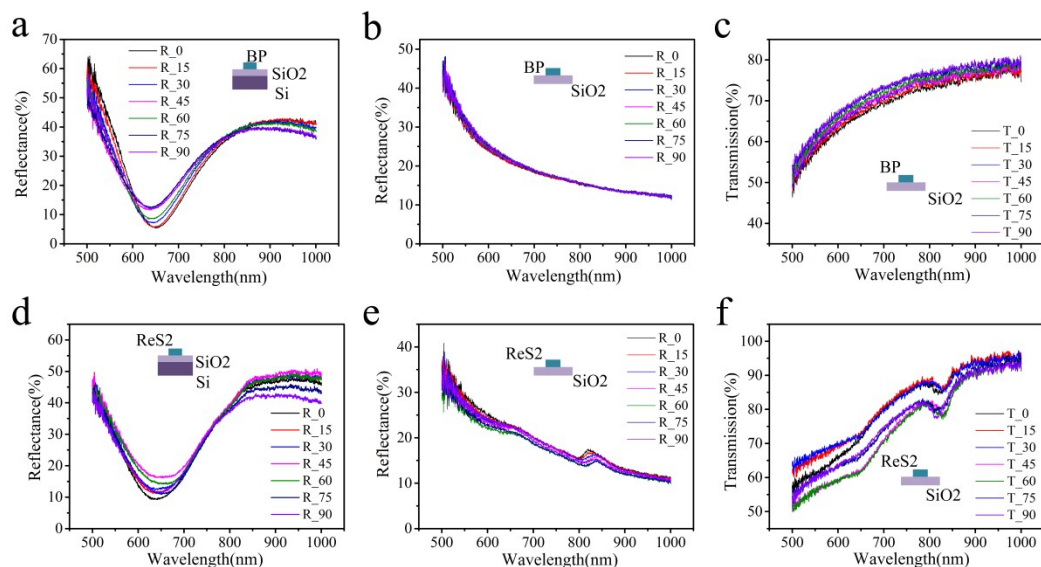


Figure S5. Optical anisotropy of BP and ReS₂ samples. **(a)-(f)** Polarization-dependent reflectance and transmission spectra for the 50 nm thick BP and ReS₂ samples on different substrates. The incident light is linearly polarized. The samples are rotated every 15°.

The spectra of BP samples have been explored a lot according latest literatures.^{3,4} However, the spectrum of ReS₂ has not been reported. Herein, we explored the transmission and reflection spectrum of BP and ReS₂ and whether it could be used for determining the crystalline orientation. As displayed in **Figure 5a** and **Figure 5d**, when the samples were exfoliated on oxide-capped silicon substrate, the reflectance spectra change significantly due to the rotation of the sample. However, when the samples were exfoliated on plates of quartz, the reflection spectra does not change even if the samples were rotated which could be observed in **Figure 5b** and **Figure 5e**. And this distinction is caused by the interlayer interference effect due to the different substrates. As illustrated in **Figure 5c** and **Figure 5f**, there is also no significant change in the transmission spectra of BP and ReS₂ when the samples were rotated due to the interference of background signal. We conclude that the reflectance and transmission spectroscopy techniques are not suitable for identifying determining the crystalline orientation of anisotropic two-dimensional materials, especially when samples are exfoliated on transparent substrate, due to the strong interference of background signal.

1. N. Mao, J. Tang, L. Xie, J. Wu, B. Han, J. Lin, S. Deng, W. Ji, H. Xu and K. Liu, *J. Am. Chem. Soc.*, 2016, **138**, 300.
2. S. Lan, S. Rodrigues, L. Kang and W. Cai, *ACS Photon.*, 2016, **3**, 1176.
3. H. Yuan, X. Liu, F. Afshinmanesh, W. Li, G. Xu, J. Sun, B. Lian, A. G. Curto, G. Ye and Y. Hikita, *Nat. Nanotechnol.*, 2015, **10**, 707.
4. C. Lin, R. Grassi, T. Low and A. S. Helmy, *Nano Lett.*, 2016, **16**, 1683.